

Post-foil interaction in the foil-induced dissociation of 3.25-MeV CH^+

I. Plessner,* E. P. Kanter, and Z. Vager*

Physics Division, Argonne National Laboratory, Argonne, Illinois 60439

(Received 27 October 1983)

The foil-induced dissociation of 3.25-MeV CH^+ is investigated by coincident detection of the fragment atoms resulting from this Coulomb explosion. The dissociation energies are deduced for both the explosion in the foil and for the post-foil interactions. The proton-carbon dissociation energies exhibit a linear dependence on the carbon charge state demonstrating a nonvarying charge state during the post-foil interaction. The data for neutral hydrogen in coincidence with carbon ions show a marked dependence of the dissociation energies on the carbon charge states. The post-foil interaction of the neutral atoms is half that of the protons. A model is suggested to explain these results.

I. INTRODUCTION

The foil-induced dissociation of fast (MeV) molecular ions has been used by several groups to provide new information about molecular-ion structures, the charge states of fast ions inside and outside solids, the interactions of such ions with the solid medium, and a variety of other atomic collision phenomena.¹ Because of the spatial and temporal correlation of the atomic fragments resulting from this "Coulomb explosion," several interesting and unique phenomena have been observed in such experiments. Many of these phenomena are now well understood, though a few outstanding problems remain. Among these problems has been some unexplained results of observations of fragments emerging from the foil in rare charge states.^{2,3} It has been suggested that some of these anomalies could be explained by the formation of dissociative molecular Rydberg states at the foil exit surface.

In this paper, we describe the results of an experiment designed to explore the formation of such Coulomb explosion fragments. In particular we have studied the proton and H^0 components resulting from the dissociation of 3.25-MeV CH^+ in a 150-Å carbon foil. By measuring the carbon charge state in coincidence with H^+ fragments, we are able to separate the Coulomb energy released during the transit time in the foil from the explosion outside the foil. The H^0 results show a sizable post-collision interaction, despite the H^0 neutrality.

In the next section we describe the Coulomb explosion process and the effects alluded to above. Section III describes the experimental measurements and Sec. IV presents the results and discussion. The conclusions are presented in Sec. V.

II. COULOMB EXPLOSIONS

When light diatomic projectiles (H_2^+ , HeH^+ , etc.) are incident at MeV energies upon a foil, most of the binding electrons of the projectile molecule are almost always totally stripped off within the first few angstroms of penetration into the solid target. The resulting two nearly

bare nuclei rapidly separate due to their mutual Coulomb repulsion, converting their initial electrostatic potential energy into kinetic energy of relative motion. This dissociation process (which proceeds with a characteristic time of $\sim 10^{-15}$ s) has been termed a Coulomb explosion.

For fast (MeV) ions in thin (~ 100 Å) foils, the Coulomb explosion produces fragments which, when observed in the laboratory frame, are measurably shifted in energy and angle.⁴ These shifts can be calculated on the basis of a simple model⁵ which assumes that inside the foil, the ionic fragments repel each other as point charges with constant effective charges determined by the stopping power of these ions. The target electrons responsible for the stopping power additionally create "wake" forces⁶ which slightly modify the pure Coulomb interaction between the ions.⁷ Additionally, multiple-scattering effects broaden the transverse velocity distributions in the foil. These effects do not appreciably affect the energy shifts. Near the target exit, the final ionic charge states are formed rapidly and the explosion runs to completion in the vacuum downstream with pure Coulomb forces between the exiting fragments.

This model of the Coulomb explosion has been sufficient in understanding most experiments which deal with both singles and coincidence measurements of the different charge components of the dissociation fragments.¹⁻⁵ Observations of rare charge states have suggested, however, significant deviations from this simple model.³ A short summary of some of these observations is given below.

(a) Extensive measurements have been performed with HeH^+ beams in the energy range of 1–4 MeV.^{4,8} The energy and angular distributions of H^+ and H^0 fragments are well described by the model discussed above. The distribution measured for H^- fragments, however, show a marked deviation from this simple picture.⁴ Surprisingly, the energy-angle distributions measured for H^- are essentially identical to the H^0 component distributions. It has been proposed that the formation of dissociative molecular Rydberg states would provide a dissociation mechanism producing such results, allowing capture of a remote electron after the He^{2+} - H^0 separation distance has in-

creased.²

(b) The zero-angle energy spectra for protons and for H^0 resulting from dissociation of 3.7-MeV OH^+ in a $3.3\text{-}\mu\text{g}/\text{cm}^2$ carbon foil⁴ show backward and forward peaks which are separated by 13.4 and 11.5 keV, respectively. The separations of these peaks calculated with the simplified model above are 12.6 and 7.0 keV.⁴ Although the proton energy separation agrees satisfactorily with the calculation, the hydrogen separation is significantly larger than the corresponding calculated value. This indicates that a post-foil repulsion occurs despite the neutrality of the H^0 fragment.

(c) Experiments have been performed in which 11.7-MeV OH^+ ions bombard targets of different thicknesses and in which proton or hydrogen fragments are detected in coincidence with the different charge states of the corresponding oxygen fragment.³ The results indicate that for thin targets the widths of the energy-integrated angular distributions of the hydrogen fragments increase with increasing charge state of the accompanying oxygen ions. Furthermore, this width, summed over all oxygen charge states, is almost independent of target thickness. The experimental difficulties in such measurements will be discussed later in this paper. These difficulties resulted in large statistical errors. Nevertheless, the results are surprising since they indicate a post-foil Coulomb repulsion between the neutral hydrogen and the oxygen fragment. As in the H^- experiment, a possible mechanism was suggested in which a remote Rydberg electron may be a spectator in the post-foil Coulomb explosion and that the hydrogen fraction would be formed through the capture of this electron by the proton, after the Coulomb explosion had continued.³

These results motivated us to design an experiment with a heavy hydride ion, similar to (c), in which the energy and angular distributions of the neutral hydrogen component could be measured (with high resolution) in coincidence with the accompanying heavy-ion charge state. The experimental difficulties posed by such measurements are described in the next section.

III. EXPERIMENT

The measurements were performed at the Argonne 4.5-MV Dynamitron using a high-resolution apparatus that has been described extensively in the literature.⁹ For this apparatus the angular and energy acceptances for a typical Coulomb explosion measurement restrict the count rate to about 10^{-5} of the total hydrogen component rate. The fraction of hydrogen component in an explosion of a hydride molecular ion beam of 1 MeV/nucleon is about 10^{-3} .¹⁰ Thus, for a coincidence measurement between hydrogen and the partner heavy ion, the count rate in the heavy-ion detector is about 10^8 times larger than the rate in the hydrogen detector. As a result, it is impractical to perform triply differential coincidence measurements (two angles and energy) in such a manner. In the experiment noted in (c) above, two position-sensitive detectors were used for the different charge states of the oxygen and for the angular distribution of the hydrogen. By sacrificing energy resolution, and measuring all angles simultaneously

an improvement in the ratio of counting rates in the two detectors of about 10^4 was achieved. This still limits the total counting rate to ~ 1 per second for all charge states and all angles. The experiment reported here overcame the above difficulties. We succeeded in measuring the energy spectra of the hydrogen component, with high resolution, for the different final charge states of the heavy partner.

A beam of 3.250-MeV CH^+ ions was collimated to 1 mm in diameter [0.11-mrad full width at half maximum (FWHM) angular divergence] and dissociated in a 150-Å-thick carbon target. The carbon (C) and the hydrogen (H) fragments were detected by two movable detectors.⁹ The C detector was a 1-mm thick plastic (pilot B) scintillator, 15-mm in diameter with a 10-mm-diam window, at a distance of 5.52 m from the target. The size of the window was chosen to be larger than the angular spread due to multiple scattering of 3.0-MeV carbon ions passing through the target. The plastic scintillator, photomultiplier tube, and electronics arrangement was capable of handling more than 10^7 carbon ions per second without detectable deterioration of rise time or pulse height. A silicon solid-state detector, collimated to 3-mm in diameter, was used for the H detection. It was mounted on a second movable arm, 5.62 m from the target. The ~ 0.6 mrad opening of the H detector is a small fraction of the typical angular spread (~ 20 mrad) of the fragments resulting from the Coulomb explosion. A set of electrostatic deflectors before and after the target⁹ were utilized in order to cleanse the beam of fragments resulting from dissociations before the foil and to spread the different charge states of C and H in the available ± 50 -mrad angular cone restricted by the flight tube.⁹ These deflectors also serve to limit the interaction region to the 6 cm between the sets of deflectors. These measurements are therefore insensitive to charge changing in the ~ 5.4 -m flight path between the post deflectors and the detectors. Spectra of the difference in the time of arrival between the protons or hydrogen to the H detector and the different charge states of carbon in the C detector were recorded. The slower rate H detector triggered the start of a time-to-pulse-height converter and the C detector provided the stop signals. Attenuating collimators were used to keep the total beam down to $\sim 10^7$ – 10^8 ions/sec.⁹

The following procedure was carried out to align the detectors. Pre-deflection and post-deflection voltages were chosen for the widest dispersion of all charge states of carbon while still maintaining the proton (hydrogen) cone within the reach of the H detector. The two-dimensional position of the H detector was optimized to be on the center of the proton (hydrogen) cone corresponding to fragments from molecules which exit the foil with their internuclear axes aligned to the beam direction. This was done by measuring the rate of the movable H detector normalized to the rate of the C detector which was held fixed. Then, for each charge state, the C detector was moved to determine an optimized position by the observation of the count rate in that detector normalized to the rate of the fixed H detector. These optimal positions were used to measure time spectra of various combinations of H-C charge states.

The connection between the time spectra and the physical parameters of the dissociative molecules is now outlined. Consider a diatomic molecular ion with constituent nuclear masses m_1 and m_2 and reduced mass μ penetrating the target with the internuclear axis aligned to the beam direction and m_1 leading m_2 . After the traversal of a length l from the target, the time delay between the two particles t_\dagger will be given by

$$t_\dagger = \frac{l}{V-v_2} - \frac{l}{V+v_1} \sim \frac{l v}{V^2},$$

where $v_1 + v_2 = v$ are the individual velocity magnitudes in the center-of-mass frame (c.m.) and V is the beam velocity ($V \gg v$).

When m_1 is the trailing particle, the difference in the time of arrival has the opposite sign and the difference between these two delay times is given by

$$\Delta t = t_1 - t_2 = \frac{2lv}{V^2} = \frac{2l(2\epsilon/\mu)^{1/2}}{V^2}, \quad (1)$$

where ϵ is the total kinetic energy in the c.m. For this experiment,

$$\Delta t(\text{nsec}) = \sqrt{306\epsilon(\text{a.u.})}. \quad (1')$$

That is, the difference between the two peaks in the time

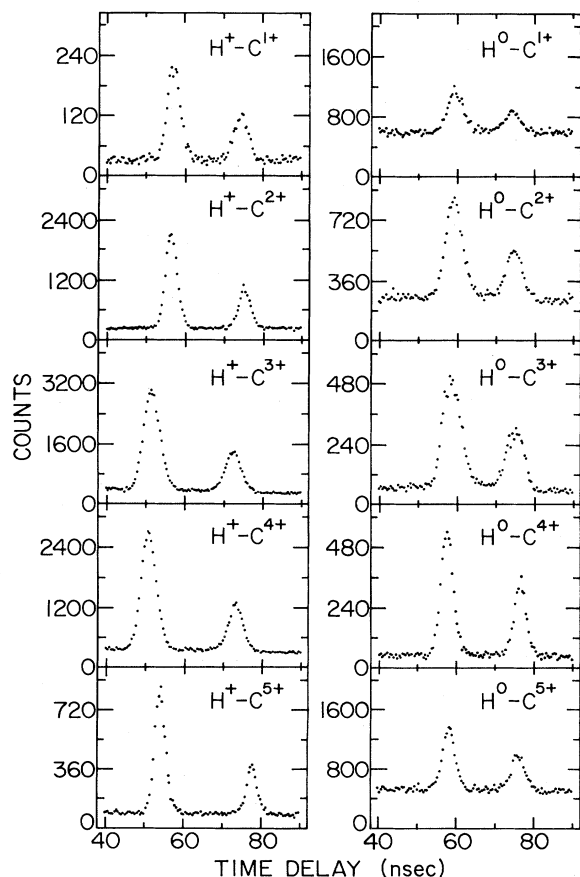


FIG. 1. Time-delay spectra for various final states emerging from the foil-induced dissociation of 3.25-MeV CH^+ .

spectrum is a direct measure of the energy released by the dissociation process. The time spectrum at zero angle provides the same information as an energy measurement of one fragment of the dissociation in coincidence with its partner. For example, a time resolution of 1 ns is equivalent to an energy measurement with ~ 0.6 keV resolution for the current experiment. For 3.25-MeV CH^+ ions incident on a $2\text{-}\mu\text{g}/\text{cm}^2$ carbon foil, the measured energy width of protons at zero angle is 2 keV.⁴ Thus the time resolution is sufficient to determine the energy released by Coulomb explosion.

IV. EXPERIMENTAL RESULTS AND DISCUSSION

The accumulated time spectra for proton- C^{q+} and hydrogen- C^{q+} coincidences, $q = 1-5$ are shown in Fig. 1. Typical accumulation times for each spectrum are 15–20 min. The ratio of “true-to-random” was adequate for accurate determinations of both peak positions and areas. Better true-to-random ratios could be obtained but were not required for these experiments.

We describe the dissociation process with a simple model. In the target, the proton acquires a c.m. kinetic energy $\epsilon_{\text{targ}}^{(p)}$ that is independent of the carbon charge states outside of the target (q). Outside the foil there is an additional energy release proportional to q . This model predicts an energy release that is linear in q ,

$$\epsilon^{(p)} = \epsilon_{\text{targ}}^{(p)} + \alpha q, \quad (2)$$

where αq represents the Coulomb energy of the fragment cluster exiting the foil. Figure 2 shows the proton- C^{q+} energy releases derived from the time spectra [see Eq. (1')] for the different charge states q of the carbon ion. Also shown is a first-order polynomial fit to the data. As expected from the simple model, the data exhibit a linear dependence on the charge state q . The experimental accuracy of the linearity can be demonstrated by the magnitude of the quadratic term [$(6 \pm 24) \times 10^{-4}$ a.u.] obtained

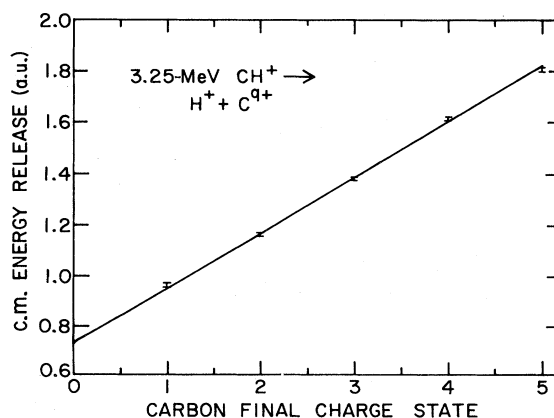


FIG. 2. c.m. energy release, as a function of the final charge state q , for the $\text{H}^+ + \text{C}^{q+}$ final states measured. The points are derived from Eq. (1) using the first moments of the peaks in the corresponding time spectra. The solid line is the result of a least-squares fit to the data.

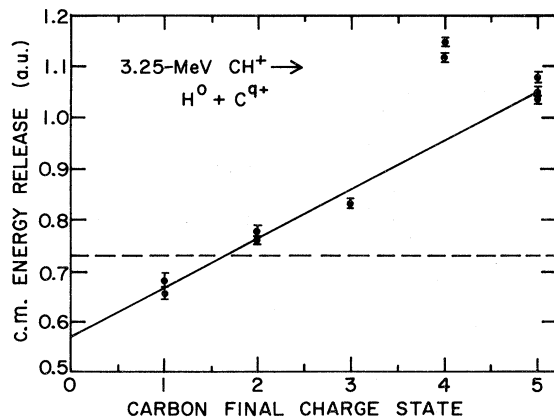


FIG. 3. c.m. energy releases, as in Fig. 2, for the $H^0 + C^{q+}$ final states. The solid line is a least-squares fit to the data, excluding the anomalous C^{4+} . The dashed line shows the energy release $\epsilon_{\text{targ}}^{(p)}$ extrapolated from the proton data.

from a second-order polynomial fit of the data. For comparison, the parameters $\epsilon_{\text{targ}}^{(p)}$ and α [see Eq. (2)] obtained from that fit are 0.731 ± 0.022 a.u. and 0.218 ± 0.015 a.u., respectively.

The observed linear dependence of the Coulomb explosion energy on the final charge state of the carbon fragment means that each charge state must be formed at the same average proton-carbon internuclear separation and hence at the same distance from the target exit surface. From the constant α quoted above, we find this average internuclear separation to be 4.59 ± 0.32 a.u. These results also imply that the carbon charge states are constant during and after the post-foil interaction. Because the carbon *KLL* Auger lifetime [$\sim 10^{-14}$ sec (Ref. 11)] is longer than the Coulomb explosion time (several femtoseconds), this finding shows that the charge-state distribution is not significantly affected by post-foil Auger processes.¹² This is in accord with measurements with 400-keV C^+ ions which find the total Auger yield per incident ion to be $\sim 10\%$ in that case.¹³

A very different phenomenon can be seen in Fig. 3 where the energy releases $\epsilon^{(H)}$ for the neutral hydrogen fragments are shown as a function of the final charge states of the accompanying carbon ions. The simple model would predict that the hydrogen component should exhibit no further energy release outside the foil and thus $\epsilon^{(H)} = \epsilon_{\text{targ}}^{(p)}$ (the dashed line in Fig. 3). This is obviously at variance with the data. It is clear that each data point of Fig. 3 is a result of a different $H-C^{q+}$ dissociative potential. Comparison to the proton results and the relation between the results for different charge states is illuminating. Several features are immediately apparent.

(a) The energy release for the $H-C^{1+}$ is *smaller* than $\epsilon_{\text{targ}}^{(p)}$, the proton energy release within the target, by 0.06 ± 0.02 a.u. Because of the well-defined separation determined earlier we reject the possibility that this decreased energy release is due to a selective hydrogen-carbon distance to form this final state. A more likely possibility is that the $H-C^+$ pair, which can form bonding states, starts exiting the foil (with kinetic energy $\epsilon_{\text{targ}}^{(p)}$) with

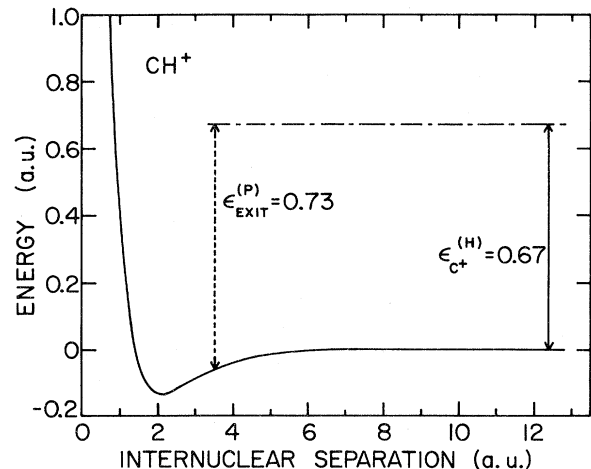


FIG. 4. Morse potential for the ground electronic state of CH^+ (with parameters from Ref. 14) to illustrate the exit separation required to produce the observed $\epsilon^{(H)}$ below $\epsilon_{\text{targ}}^{(p)}$ for $H^0 + C^{1+}$.

a potential energy below the potential level¹⁴ at infinite distance (see Fig. 4). The final kinetic energy will therefore be decreased by the attractive potential upon exit. For the electronic ground state of CH^+ , the internuclear separation at exit required to fit the data would be $3.5_{-0.3}^{+0.5}$ a.u.

(b) In general, the released energy increases with the carbon charge state. This means that a good portion of the proton- C^{q+} Coulomb repulsion is not screened. A comparison of the average slope in Fig. 3 to the slope of Fig. 2 could be used as a measure of the unscreened Coulomb repulsion.

A simple model for visualizing such partial screening is to consider an electron orbiting around the carbon at a radius R and a pure Coulomb interaction between the proton- C^{q+} cluster until the internuclear distance reaches R . Then, either the proton picks up the electron (probability $\sim 10^{-3}$) and stops the Coulomb repulsion, or there is no pickup and the Coulomb repulsion continues. Comparing the slopes of the fitted lines, we find $R \sim 9$ a.u.

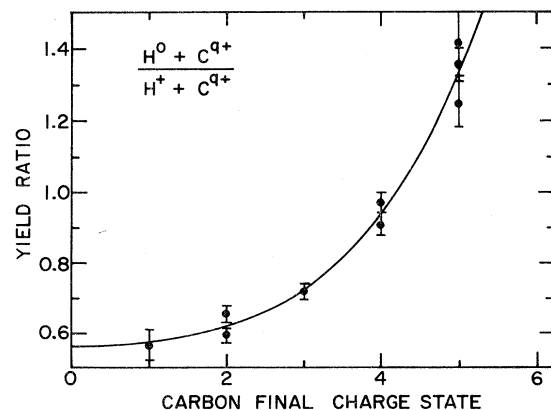


FIG. 5. Yield ratios W_q^0/W_q^{1+} as a function of the charge state q . The calculation of the W 's is described in the text. The solid line is drawn to guide the eye.

(c) There seems to be a "shell-effect" in the larger energy release (Fig. 2) for the C^{4+} in comparison with the other charge states. The possibility of less screening for C^{4+} is appealing but clearly indicates the drawback of the simple Rydberg electron model.

Another aspect of these data can be seen in the comparison of the distributions of carbon charge states accompanying either a proton or a hydrogen atom. In order to extract such information from the data shown in Fig. 1, the integrals under the leading peaks (proton leading) were multiplied by the squares of the time separations. The leading peaks are used to minimize the complications due to wake forces.⁶ The scaling factor is necessary to account for the Jacobian transforming the yields to the center-of-mass (c.m.) system.⁸ These scaled integrals were normalized to the total number of the counts in the H detector to give the quantities W_q^0 and W_q^{1+} which represent the charge distributions for the respective C^{q+} -H or C^{q+} -p pairs. The W 's closely approximate the total yield in the c.m. system. The ratios W_q^0/W_q^{1+} are plotted in Fig. 5 as a function of q . It is clear that the charge distribution accompanying neutral hydrogen fragments strongly favors higher charge states. This result runs contrary to the simple intuition that in the competition between the C^{q+} and the proton for capturing a loose electron, the carbon should succeed more easily because of its higher charge state. On the other hand, this supports the idea that hydrogen atoms coming from such an explosion can be created only if there are loose electrons in the vicin-

ity. The carbon ions with higher charge states attract more loose electrons than do those ions of lower charge state¹⁵ and thus will enhance the probability of H^0 formation.

V. CONCLUSION

The comparison between dissociation energies and yields as a function of the charge state of the heavier partner was found to be illuminating in several respects. There is no evidence for post-foil Auger processes affecting the carbon charge state. The production of hydrogen atoms near the carbon partner goes only via a pickup of an electron attached to the C-H couple. This is evident from the strong dependence of the relative hydrogen yield on the carbon charge state. The remnant of charge-state dependence of the Coulomb explosion with the hydrogen partner indicates that the distance at which electron capture occurs is roughly 5 Å. Lastly, the shell closure for C^{4+} appears to increase the dissociation energy acquired by hydrogen fragments above the systematic trend of the other charge states.

ACKNOWLEDGMENTS

We wish to acknowledge the assistance of B. Orszula in conducting these measurements. This research was supported by the U.S. Department of Energy, Office of Basic Energy Sciences, under Contract No. W-31-109-Eng-38.

*Permanent address: Weizmann Institute of Science, Rehovot 76100, Israel.

¹See, e.g., E. P. Kanter, *Comments At. Mol. Phys.* **11**, 63 (1981) and references therein; J. Remillieux, *Nucl. Instrum. Methods* **170**, 31 (1980); D. S. Gemmell, *ibid.* **170**, 41 (1980); R. Laubert, *IEEE Trans. Nucl. Sci.* **NS-26**, 1020 (1979).

²D. S. Gemmell, *Nucl. Instrum. Methods* **194**, 255 (1982).

³A. Faibis, G. Goldring, M. Hass, R. Kaim, I. Plessner, and Z. Vager, *Nucl. Instrum. Methods* **194**, 299 (1982).

⁴P. J. Cooney, D. S. Gemmell, W. J. Pietsch, A. J. Ratkowski, Z. Vager, and B. J. Zabransky, *Phys. Rev. A* **24**, 746 (1981).

⁵E. P. Kanter, in *Molecular Ions*, edited by J. Berkowitz and K.-O. Groeneveld (Plenum, New York, 1983), p. 463.

⁶Z. Vager and D. S. Gemmell, *Phys. Rev. Lett.* **37**, 1352 (1976).

⁷D. S. Gemmell, J. Remillieux, J.-C. Poizat, M. J. Gaillard, R. E. Holland, and Z. Vager, *Phys. Rev. Lett.* **34**, 1420 (1975).

⁸E. P. Kanter, P. J. Cooney, D. S. Gemmell, K.-O. Groeneveld, W. J. Pietsch, A. J. Ratkowski, Z. Vager, and B. J. Zabransky, *Phys. Rev. A* **20**, 834 (1979).

⁹B. J. Zabransky, P. J. Cooney, D. S. Gemmell, E. P. Kanter, and Z. Vager, *Rev. Sci. Instrum.* **54**, 531 (1983).

¹⁰M. J. Gaillard, J.-C. Poizat, A. Ratkowski, J. Remillieux, and M. Auzas, *Phys. Rev. A* **16**, 2323 (1977).

¹¹E. J. McGuire, *Phys. Rev. A* **185**, 1 (1969).

¹²H. D. Betz and L. Grodzins, *Phys. Rev. Lett.* **25**, 211 (1970).

¹³R. A. Baragiola, P. Ziem, and N. Stolterfoht, *J. Phys. B* **9**, L447 (1976).

¹⁴G. Herzberg, *Spectra of Diatomic Molecules* (Van Nostrand Reinhold, New York, 1950).

¹⁵V. S. Nikolaev, *Usp. Fiz. Nauk* **85**, 679 (1965) [*Sov. Phys.—Usp.* **8**, 269 (1965)].